ELSEVIER

www.elsevier.nl/locate/jorganchem

Journal of Organometallic Chemistry 601 (2000) 34–42

Journal of Organometallic Chemistry

From molecules to aggregates: crystal structures of molybdenum binuclear complexes

Patrícia Pinto [a], Eva Barranco [a], Maria José Calhorda [a,b,*], Vitor Félix [a,c], Michael G.B. Drew [d]

[a] *Instituto de Tecnologia Química e Biológica (ITQB), Quinta do Marquês, EAN, Apt 127, 2781-901 Oeiras, Portugal*
[b] *Departamento de Química e Bioquímica, Faculdade de Ciências da Universidade de Lisboa, 1749-016 Lisbon, Portugal*
[c] *Departamento de Química, Universidade de Aveiro, 3810-193 Aveiro, Portugal*
[d] *Department of Chemistry, University of Reading, Whiteknights, Reading RG6 6AD, UK*

Received 15 November 1999; received in revised form 21 December 1999

Abstract

The new complexes $[MoCl(\eta^3\text{-}C_3H_5)(CO)_2(H_2biim)]$, $[N^nBu_4][\{Mo(\eta^3\text{-}C_3H_5)(CO)_2\}_2(\mu\text{-}Cl)_2(\mu\text{-}OMe)]$, and $[PPN][\{Mo(\eta^3\text{-}C_3H_5)(CO)_2\}_2(\mu\text{-}Cl)_3]$ (PPN is $Ph_3P{=}N^+{=}PPh_3$) were synthesized and the two binuclear compounds were characterized by single-crystal X-ray diffraction. Although an anion $[\{Mo(\eta^3\text{-}C_3H_5)(CO)_2\}_2(\mu\text{-}Cl)_3]^-$ has been described in the literature, being formed both in solution and in the solid, another conformer was present in the crystal of $[PPN][\{Mo(\eta^3\text{-}C_3H_5)(CO)_2\}_2(\mu\text{-}Cl)_3]$, exhibiting an eclipsed arrangement of the allyl groups. The same arrangement was found for the $[\{Mo(\eta^3\text{-}C_3H_5)(CO)_2\}_2(\mu\text{-}Cl)_2(\mu\text{-}OMe)]^-$ anion. Cyclic voltammetry data show that the eclipsed conformer of $[\{Mo(\eta^3\text{-}C_3H_5)(CO)_2\}_2(\mu\text{-}Cl)_3]^-$ remains in solution, as the other one, with staggered allyl groups, is formed when dissolving the parent compound $[MoCl(\eta^3\text{-}C_3H_5)(CO)_2(NCMe)_2]$ and exhibits a distinctive pattern. Density functional theory (DFT) calculations showed the two conformers to have very similar energies, both for this and for the related anion $[\{Mo(\eta^3\text{-}C_3H_5)(CO)_2\}_2(\mu\text{-}Cl)_2(\mu\text{-}OMe)]^-$. The crystal structure of $[PPN][\{Mo(\eta^3\text{-}C_3H_5)(CO)_2\}_2(\mu\text{-}Cl)_3]$ exhibits double channels formed by the PPN cation which are occupied by chains of the binuclear anions.

Keywords: Molybdenum; DFT calculations; Allyl complexes; Crystal structures; Binuclear complexes

1. Introduction

Organometallic complexes are very versatile species, which can be used as building blocks to design molecular solids [1]. Their main advantage over more traditional organic precursors lies in their increased versatility. Indeed, a change in metal allows the coordination sphere to vary as well, leading to different shapes and charges for the complex, which may have a determining effect in a crystallization process. Moreover, reduction or oxidation reactions can be undergone by many metal centers, changing the electronic richness of the metal but not, in many cases, the stoichiometry of the complex. Units containing more than one metal atom are even more interesting, if the communication between those metal centers can be turned on or off by redox processes or some other method. This behavior holds a high potential for applications in many fields.

In an attempt to understand the factors responsible for the properties of solids, binuclear complexes were used as precursors. The metal atoms may be linked by bridging ligands or exhibit an unsupported metal–metal bond. In many binuclear complexes, where the metal centers are connected by bridging ligands, such as $Fe_2(CO)_9$, the existence of a metal–metal bond has been discussed widely, as it is required in order for each metal to achieve a formal 18 electron count [2]. In other examples, the metal centers are saturated, the metal–metal distances are long, so that there is no direct interaction between them. In this work, using as a precursor the well-known allyl complex $[MoCl(\eta^3\text{-}C_3H_5)(CO)_2(NCMe)_2]$ [3], we introduce two complexes

* Corresponding author. Fax: +351-21-4411277.
E-mail address: mjc@itqb.unl.pt (M.J. Calhorda)

0022-328X/00/$ - see front matter
PII: S0022-328X(00)00018-8

of this latter family, containing either three chloride or two chloride and one methoxy bridges, describe their crystal structures, and discuss their electronic structure.

2. Results and discussion

2.1. Chemical results

The allyl complex $[MoCl(\eta^3\text{-}C_3H_5)(CO)_2(NCMe)_2]$ (**1**) [3] has been used widely as a convenient source of molybdenum(II) derivatives, because it contains two labile nitrile ligands. The reaction with 2,2′-biimidazole (H_2biim) led to the substitution of the two nitriles, to afford a neutral $[MoCl(\eta^3\text{-}C_3H_5)(CO)_2(H_2biim)]$ complex (**2**), similar to the known 2,2′-bipyridyl and phenanthroline derivatives, which could also be obtained in this way [4]. The IR spectrum exhibits the $\nu_{C\equiv O}$ stretching modes at 1944 and 1854 cm^{-1} and some new ones, assigned to the coordinated 2,2′-bisimidazole. The ^{1}H-NMR spectrum shows one broad peak for this ligand ($\delta = 7.48$), and three allyl peaks at $\delta = 4.09$, 3.53, and 1.41, integrating as 4:1:2:2, respectively. This complex is extremely insoluble, which prevented its recrystallization and cocrystallization with suitable H-bond acceptors to interact with the two N–H groups. On the other hand, deprotonation of the coordinated ligand leads to a new organometallic ligand with two nitrogen donor atoms $[MoCl(\eta^3\text{-}C_3H_5)(CO)_2(biim)]^{2-}$, which can be used to prepare binuclear complexes by reaction with, among others, the molybdenum precursor **1**. The same reaction can be achieved by direct reaction of $[MoCl(\eta^3\text{-}C_3H_5)(CO)_2(NCMe)_2]$ with the lithium bisimidazolato, stabilized by TMEDA. Attempts to grow crystals of the resulting product led to orange–greenish crystals, which did not contain the nitrogen ligand. Their formulation was determined by means of single-crystal X-ray diffraction as $[N^nBu_4]$-$[\{Mo(\eta^3\text{-}C_3H_5)(CO)_2\}_2(\mu\text{-}Cl)_2(\mu\text{-}OMe)]$ (**3**) (see below). The IR spectrum of this complex exhibits the typical $\nu_{C\equiv O}$ stretching modes at 1921 and 1809 cm^{-1}, shifted by 23 and 44 cm^{-1} relative to those of the parent compound, as well as bands assigned to the C–H vibrations at 2962, 2875, and 2808 cm^{-1}. The peaks in the ^{1}H-NMR spectrum could not be assigned fully, as the large number of protons belonging to the N^nBu_4 counter ion cover the allylic protons.

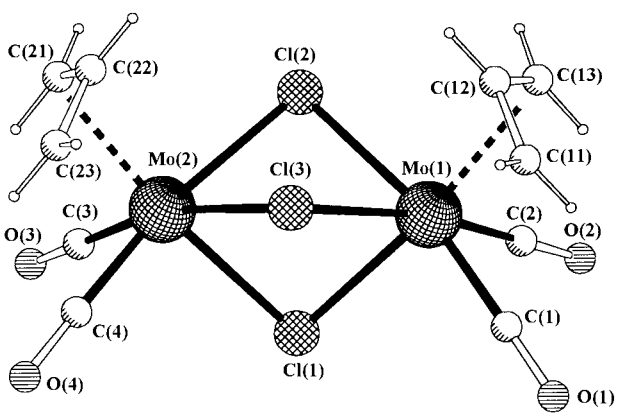

Fig. 1. A PLUTON view of the binuclear anion $[\{Mo(\eta^3\text{-}C_3H_5)(CO)_2\}_2(\mu\text{-}Cl)_3]^-$ (**4**$^-$) with the atomic numbering scheme adopted.

A related anionic binuclear complex, [PPN][$\{Mo(\eta^3\text{-}C_3H_5)(CO)_2\}_2(\mu\text{-}Cl)_3$] (**4**), was obtained upon recrystallization of the product from the reaction between $[MoCl(\eta^3\text{-}C_3H_5)(CO)_2(NCMe)_2]$ and $[Au_2Cl_2PPN]$ (PPN is $Ph_3P{=}N^+{=}PPh_3$) and its nature elucidated by single-crystal X-ray diffraction. The two $\nu_{C\equiv O}$ stretching modes were observed at 1861 and 1928, 1950 cm^{-1}, with the strongest C–H stretching frequency at 3057 cm^{-1}. For this complex, the peaks of the allyl ligand are well separated from those of phosphines of the counterion in the ^{1}H-NMR spectrum. Anions with this composition have been described before [5], but the spectroscopic data (IR and ^{1}H-NMR) are different. We shall discuss these aspects later.

2.2. Crystallography

The crystal structures of complexes $[N^nBu_4][\{Mo(\eta^3\text{-}C_3H_5)(CO)_2\}_2(\mu\text{-}Cl)_2(\mu\text{-}OMe)]$ (**3**) and [PPN][$\{Mo(\eta^3\text{-}C_3H_5)(CO)_2\}_2(\mu\text{-}Cl)_3$] (**4**) were determined by X-ray diffraction analysis. The unit cell of complex **4** is built up from an asymmetric unit composed of one dimeric anion $[\{Mo(\eta^3\text{-}C_3H_5)(CO)_2\}_2(\mu\text{-}Cl)_3]^-$ (**4**$^-$), and one cation $[Ph_3P{=}N^+{=}PPh_3]$.

The crystal structure of complex **3** consists of the dimeric anion $[\{Mo(\eta^3\text{-}C_3H_5)(CO)_2\}_2(\mu\text{-}Cl)_2(\mu\text{-}OMe)]$ (**3**$^-$) and the $[N^nBu_4]^+$ cation, which is strongly disordered. All attempts to find a disorder model for $[N^nBu_4]^+$ were unsuccessful (see below) and a detailed analysis of the structural features of complex **3** is as a consequence limited. However, the structure of complex anion is determined unequivocally, provides a detailed characterization of the coordination sphere of two metal centers, and allows a broader discussion of the conformational features of the apparently flexible $[\{M(\eta^3\text{-allyl})(CO)_2\}_2(\mu\text{-}X)_3]^-$ species (M = Mo(II) or W(II)) [5,6]. For comparison purposes, the molecular structures of the two related binuclear anions **4**$^-$ and **3**$^-$ will be discussed together.

Molecular diagrams, including the crystallographic labeling schemes, are shown in Figs. 1 and 2 for binuclear anions **4**$^-$ and **3**$^-$, respectively. Selected bond lengths and angles are listed in Table 1.

In both complexes, each molybdenum center is coordinated to two carbonyl groups and one allyl ligand in a η^3-mode. The two independent $Mo(\eta^3\text{-}C_3H_5)(CO)_2$ moieties are bridged by three chlorine atoms in **4**$^-$ and

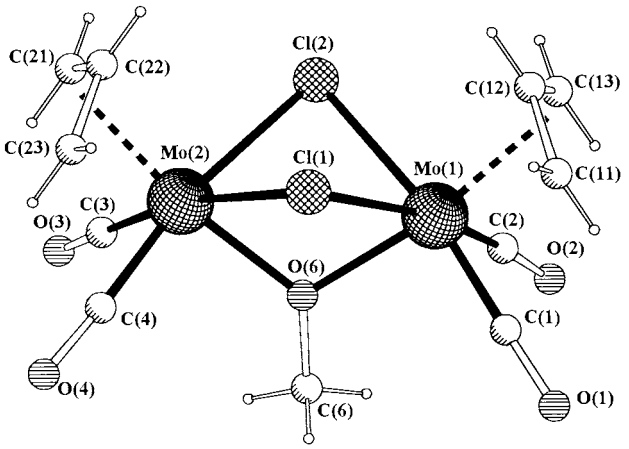

Fig. 2. A PLUTON view of the binuclear anion $[\{Mo(\eta^3\text{-}C_3H_5)(CO)_2\}_2(\mu\text{-}Cl)_2(\mu\text{-}OMe)]^-$ ($\mathbf{3}^-$) with the atomic numbering scheme adopted.

Table 1
Selected bond lengths (Å) and angles (°) for $[N^nBu_4][\{Mo(\eta^3\text{-}C_3H_5)(CO)_2\}_2(\mu\text{-}Cl)_2(\mu\text{-}OMe)]$ (**3**) and $[PPN][\{Mo(\eta^3\text{-}C_3H_5)(CO)_2\}_2(\mu\text{-}Cl)_3]$ (**4**) [a]

Complex	**3** [X = O(6)]	**4** [X = Cl(3)]
Bond lengths		
Mo(1)–Cl(1)	2.653(5)	2.536(4)
Mo(1)–Cl(2)	2.619(5)	2.603(4)
Mo(1)–X	2.111(12)	2.596(4)
Mo(2)–Cl(1)	2.655(5)	2.570(4)
Mo(2)–Cl(2)	2.633(5)	2.608(4)
Mo(2)–X	2.098(13)	2.572(4)
Mo(1)–$C_{carbonyl}$	1.89(3)	1.95(1)
Mo(2)–$C_{carbonyl}$	1.92(3)	1.95(2)
Bond angles		
$C_{carbonyl}$–Mo(1)–$C_{carbonyl}$	78.1(1)	78.5(6)
$C_{carbonyl}$–Mo(2)–$C_{carbonyl}$	78.3(1)	78.8(7)
Mo(1)–C=O	174(3)	178(1)
Mo(2)–C=O	178(3)	179(1)
Cl(1)–Mo(1)–Cl(2)	79.5(7)	77.2(1)
Cl(1)–Mo(1)–X	73.6(4)	78.6(1)
X–Mo(1)–Cl(2)	75.5(4)	79.8(1)
Cl(1)–Mo(2)–X	73.7(4)	78.4(1)
Cl(1)–Mo(2)–Cl(2)	81.0(2)	76.5(1)
X–Mo(2)–Cl(2)	75.4(4)	80.2(1)
Mo(1)–Cl(1)–Mo(2)	78.9(2)	87.4(1)
Mo(1)–Cl(2)–Mo(2)	79.9(2)	85.2(1)
Mo(2)–X–Mo(1)	106.5(5)	86.1(1)

[a] The bond lengths and angles involving the carbonyl groups are average values.

by two chlorine atoms and one methoxy group in $\mathbf{3}^-$, giving rise to a pseudo-octahedral geometry around each molybdenum atom. The overall geometry can be described as a distorted confacial bioctahedron, with the centroids of the allyl ligands occupying two sites of this coordination polyhedron. The face shared by the two octahedra is defined by the three bridging ligands.

The average metal-to-C3centroid distances are 2.036 and 2.040 Å for complexes $\mathbf{4}^-$ and $\mathbf{3}^-$, respectively. In the coordination sphere of $\mathbf{3}^-$, the two allyl ligands are *trans* to the methoxy group leading to angles between the C3centroid and oxygen atom O(6) of 169.5 and 170.3°, respectively. In complex **4**, the average value of the two Mo–Cl distances involving the bridging chlorine Cl(1) [2.553(4) Å], *trans* to the allyl ligands, is slightly shorter than that involving the other two chlorine bridges, *trans* to the carbonyl ligands [2.595(4) Å]. Average Mo–Cl distances in $\mathbf{3}^-$ are 2.640(5) Å, average Mo–CO bond distances are 1.95(2) Å in $\mathbf{4}^-$ and 1.90(5) in $\mathbf{3}^-$, while the corresponding OC–Mo–CO angles are 78.6(6)° in $\mathbf{4}^-$ and 78.2(1)° in $\mathbf{3}^-$. The carbonyl groups are coordinated linearly to the molybdenum atoms, the average Mo–C–O angles being 178(1) and 176(3)°, for $\mathbf{4}^-$ and $\mathbf{3}^-$, respectively. These geometries agree well with those found for the anion $\mathbf{4}^-$ in the complex $[Mo(CO)_2(\eta^3\text{-}C_3H_5)(MeCN)_3][\{Mo(\eta^3\text{-}C_3H_5)(CO)_2\}_2(\mu\text{-}Cl)_3]$ (**5**) [5] and $[\{W(\eta^3\text{-}C_3H_5)(CO)_2\}_2(\mu\text{-}Cl)_3]^-$ anion ($\mathbf{6}^-$) [6], although different isomers are present, as will be discussed further below.

The Mo–O(bridge) distances of 2.111(12) and 2.098(13) Å in $\mathbf{3}^-$ are similar to those found for the binuclear complex $[\{Mo(\eta^7\text{-}C_7H_7)\}_2(\mu\text{-}Cl)_2(\mu\text{-}OH)]^-$ (**7**), where the two molybdenum centers are also bridged by one oxygen and two chlorine atoms [7]. Cotton and Ucko introduced several structural parameters to characterize the geometric distortions in bioctahedral structures such as those discussed above [8]. Among them, the parameter $\beta - 70.53°$ reflects the axial distortion, away from the octahedron, of the central core of $[\{Mo(C3centroid)(CO)_2\}_2(\mu\text{-}Cl)_3]$ in $\mathbf{4}^-$ and $[\{Mo(C3centroid)(CO)_2\}_2(\mu\text{-}Cl)_2(\mu\text{-}OMe)]$ in $\mathbf{3}^-$ along the axis defined by the two metal centers. β is the M–L–M bond angle (L = Cl or OMe) and takes the value of 70.53° for an ideal confacial bioctahedron. Thus, $\beta - 70.53°$ is equal to 0° for an ideal bioctahedral structure. Negative and positive values will be expected for contracted and elongated bioctahedral structures, respectively. Negative values for the $\beta - 70.53°$ parameter should be helped by the formation of a metal–metal bond, while positive values reflect the absence of such interactions. For the anion $\mathbf{4}^-$, values of 16.9(1), 14.7 (1) and 15.6(1)° for the $\beta - 70.53°$ parameter and a Mo···Mo distance of 3.526(1) Å were found. In anion $\mathbf{3}^-$, the $\beta - 70.53°$ parameter has the small values of 8.4(1) and 9.4(2)°, calculated here from the two Mo–Cl–Mo angles. The Mo···Mo distance of 3.372(2) Å is 0.15 Å shorter than for $\mathbf{4}^-$. The binuclear anions $[\{M(\eta^3\text{-}C_3H_5)(CO)_2\}_2(\mu\text{-}Cl)_3]^-$ [M = Mo(II) or W(II)] in complexes **5** and **6** have $\beta - 70.53°$ parameters [14.5, 16.5 and 16.5° in **5** and 16.5, 17.5 and 18.5° in **6**] and M···M distances [3.531 Å in **5** and 3.539 Å in **6**] similar to those found for anion $\mathbf{4}^-$ [5,6]. Therefore, this analysis suggests the absence of metal–metal (M = Mo(II) or M = W(II)) bonds in these anionic com-

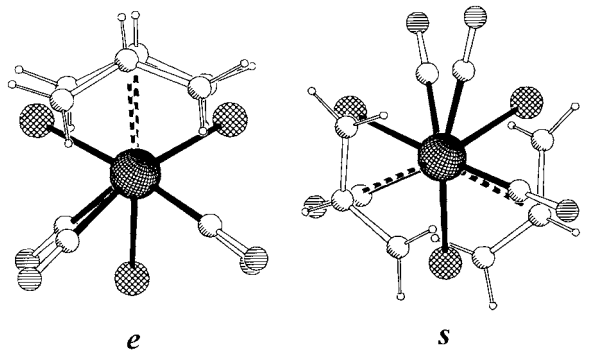

Fig. 3. The two conformations adopted by the [{Mo(η^3-C_3H_5)$(CO)_2$}$_2$(μ-Cl)$_3$]$^-$ anion in complexes **4** and **5**: eclipsed (*e*, left) and staggered (*s*, right).

plexes, in agreement with the formal 18 electron count for each d^2 metal atom. In fact, the four Mo···Mo distances reported for these complex anions are clearly too long to be ascribed to molybdenum–molybdenum bonds.

The relative orientation of the two allylic fragments in each binuclear unit can be characterized by the rotation angle (λ) defined by the centroids of these ligands and the two molybdenum atoms. When the centroids are eclipsed fully along the Mo–Mo vector, the λ angle will be 0°, while the *trans* staggered arrangement will lead to a λ angle of 180°. λ takes the values of 5.0° in **4**$^-$ and 6.9° in **3**$^-$, indicating that, in the complexes under study, the two allyl ligands are almost eclipsed. Interestingly, both anion **4**$^-$ in complex **5** and anion **6**$^-$ in complex **6** exhibit intermediate conformations with λ angles of 127.6 and 117.6°, respectively. Fig. 3 shows the two conformations adopted by the complex anion [{Mo(η^3-C_3H_5)$(CO)_2$}$_2$(μ-Cl)$_3$]$^-$ in **4** and **5**.

2.3. Voltammetric studies

The cyclic voltammetry of solutions of the binuclear complexes **4** and **3** was studied in several solvents, as well as that of **2**, and the precursor **1** for comparison. [MoCl(η^3-C_3H_5)$(CO)_2(NCMe)_2$] (**1**) has been shown to exhibit one quasi-reversible wave in MeCN, while three waves are observed in CH_2Cl_2. These differences have been traced to the lability of the nitrile ligands, which lead to the formation of two different complexes, assigned as [{Mo(η^3-C_3H_5)$(CO)_2$}$_2$(μ-Cl)$_3$]$^-$ and [Mo(η^3-C_3H_5)$(CO)_2(NCMe)_3$]$^+$ [9]. The first is apparently the same anion as in **3**.

The results of cyclic voltammetry in MeCN and CH_2Cl_2 (see details in Section 4) are collected in Table 2 and are comparable to those obtained for **1** in a published study [9].

Indeed, the same quasi-reversible process is observed in MeCN, as well as three processes in CH_2Cl_2. The $E_{1/2}$ values differ because a different reference electrode is being used. On the other hand, none of the waves observed in the cyclic voltammogram of **4** coincides with those of **1**, showing that the anion **4**$^-$ present in solution is not the same as that formed by the dissociation of **1** in CH_2Cl_2. The previous results from the crystal-structure determination suggest that the conformer formed upon dissolving **4** is the eclipsed, as found in the crystal, while dissociation of **1** leads to the staggered conformer. This will be discussed again in the next section. The effect of substituting the Cl bridging ions by a methoxide can be detected in the cyclic voltammogram. Indeed, both solutions exhibit a quasi-reversible wave (only the $E_{1/2}$ values differ from one solvent to the other) and other two irreversible oxidations not showing their counterpart. The absence of this counterpart is more pronounced in **3** than in **4**. The $E_{1/2}$ values cannot be compared, as the order is inverted when the solvent changes. Finally, the 2,2′-bisimidazole complex **2** can be compared with the bipy and phen

Table 2
Cyclic voltammetric data for the allyl complexes **1**, **2**, **3**$^-$, and **4**$^-$

Complex	CH_2Cl_2			NCMe		
	$E_{1/2}$	ΔE	i_{pa}/i_{pc}	$E_{1/2}$	ΔE	i_{pa}/i_{pc}
[MoCl(η^3-C_3H_5)$(CO)_2(NCMe)_2$] (**1**)	555	118	0.97	6647	83	1.05
	962	107				
	1120	99				
[{Mo(η^3-C_3H_5)$(CO)_2$}$_2$(μ-Cl)$_2$(μ-OMe)]$^-$ (**3**$^-$)	560	64	1.0	631	62	0.97
	910 [a]			820 [a]		
	1164 [a]			1070	84	1.03
[{Mo(η^3-C_3H_5)$(CO)_2$}$_2$(μ-Cl)$_3$]$^-$ (**4**$^-$)	588	72	1.86	625	62	1.13
[MoCl(η^3-C_3H_5)$(CO)_2(H_2biim)$] (**2**)	494	88	1.78	881	34	1.82
				436 [b]		

[a] Only E_a.
[b] Only E_c.

Table 3
Relative energies of the two isomers of $[\{Mo(\eta^3\text{-}C_3H_5)(CO)_2\}_2(\mu\text{-}Cl)_2(\mu\text{-}X)]^-$ (X = Cl, OMe) in kcal mol^{-1}

Complex	Eclipsed (*e*)	Staggered (*s*)
$[\{Mo(\eta^3\text{-}C_3H_5)(CO)_2\}_2(\mu\text{-}Cl)_3]^-$ (**4**$^-$)	+0.35	0
$[\{Mo(\eta^3\text{-}C_3H_5)(CO)_2\}_2(\mu\text{-}Cl)_2(\mu\text{-}OMe)]^-$ (**3**$^-$)	0	+0.58

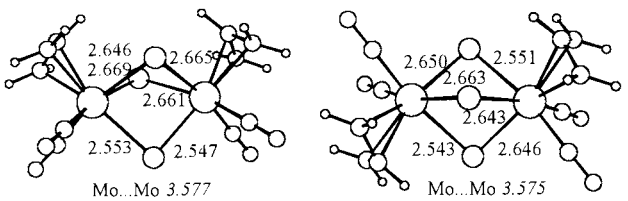

Fig. 4. DFT optimized structures of the $[\{Mo(\eta^3\text{-}C_3H_5)(CO)_2\}_2(\mu\text{-}Cl)_3]^-$ anion in the two conformations: eclipsed (*e*, left) and staggered (*s*, right).

derivatives described in the literature [9], as the ligand also binds through two nitrogen atoms. For $[\{MoCl(\eta^3\text{-}C_3H_5)(CO)_2(L\text{-}L)Cl]$ (L–L = bipy, phen) one single one-electron oxidation has been observed and assigned to a quasi-reversible process. When L–L = 2,2′-bisimidazole, there is one irreversible, but complete, wave (the i_{pa}/i_{pc} ratio is ca. 1.8), as well as two other incomplete processes, in MeCN. The poor solubility in CH_2Cl_2 prevented any voltammogram being obtained.

2.4. Theoretical calculations

The observation of more than one isomer of the anion $[\{Mo(\eta^3\text{-}C_3H_5)(CO)_2\}_2(\mu\text{-}Cl)_3]^-$ (**4**$^-$) in different complexes, led us to perform density function theory (DFT) calculations [10] (ADF program [11], see Section 4 for details) in order to find out their relative stability and to explore the possibility of the existence of isomers for the other anionic complex $[\{Mo(\eta^3\text{-}C_3H_5)(CO)_2\}_2(\mu\text{-}Cl)_2(\mu\text{-}OMe)]^-$ (**3**$^-$).

It was seen in Fig. 3 that one isomer exhibits an eclipsed conformation of the two allyls. The threefold kind of symmetry, typical of the pseudo octahedral arrangement, can in principle lead to three isomers, for λ 0, 120, and 240°, respectively. The symmetry of the anions **4**$^-$ and **3**$^-$, however, allows only two independent isomers. If one allyl is allowed to rotate by ca. 120° relative to the other, the structure of these anions is observed. Further rotation of 120° leads to an identical arrangement. There are only two isomers, which will be described as eclipsed and staggered for clarity. The relative energies given in Table 3 result from a full geometry optimization without any symmetry constraints.

The differences in energy are extremely small, especially for the complex with three chlorine bridges. It is therefore not surprising that both isomers have been found. Packing effects will be important in adding to the stability of either form, the overall stability depending also on the counter ion. For the second complex, only one compound is known and it adopts the arrangement with the lowest energy. As the two isomers were characterized structurally for the derivatives of $[\{Mo(\eta^3\text{-}C_3H_5)(CO)_2\}_2(\mu\text{-}Cl)_3]^-$, **4** and **5**, respectively, they will be used to compare and discuss the results of the calculations, as for the OMe bridged complex only one, poor quality, crystal structure is available.

We emphasize in Fig. 4 the most important details relative to the two structures. The Mo–Cl distances were all different, owing to the lack of symmetry constraints in the calculation, respectively, 2.650, 2.646 Å in *s*, 2.553, 2.547 Å in the eclipsed form *e*, for the Mo–Cl bond *trans* to the allyl ligands, and 2.543, 2.551, 2.663, 2.643 Å in the staggered form *s*, 2.646, 2.665, 2.669, 2.661 Å in *e* for the others. The Mo–Mo distance was found to be 3.575 and 3.577 Å in *s* and *e*, respectively. These results show a good agreement with experimental distances, the calculated root mean square (r.m.s.) values, excluding hydrogen atoms, between the X-ray structure of **4**$^-$ and *cis*-**4**$^-$ being 0.078 Å, and between the X-ray structure of **5**$^-$ and *trans*-**4**$^-$ 0.064 Å. The r.m.s. value calculated for the X-ray structure of **3**$^-$ and *cis*-**3**$^-$ is larger (0.120 Å), owing to the poor quality of the structure, but still reflects a good agreement. The energy differences are very small and difficult to interpret, but show that both isomers correspond to local minima. We can, therefore, believe that each isomer may be formed depending on the conditions, the staggered form being the thermodynamic product obtained by dissociation of the mononuclear precursor in CH_2Cl_2, while the serendipitous synthesis of our binuclear complex **4** resulted in the less stable eclipsed form, owing probably to kinetic reasons.

We also calculated the energy differences between the anions and the oxidized neutral species, which are, respectively, 3.83 eV for *cis*-**4**$^-$, 3.81 eV for *trans*-**4**$^-$, and 3.75 eV for *cis*-**3**$^-$, in order to compare their relative oxidation potentials, but the differences are rather small. It is not surprising that the change in solvent can invert the order, as found between *cis*-**4**$^-$ and *cis*-**3**$^-$. The difference between *cis*-**4**$^-$ and *trans*-**4**$^-$ is also small. However, the strong solvent dependence restricts the value of such comparisons.

2.5. The crystal structures

After having studied the isolated anions, we shall now examine their crystal structures, in an effort to understanding the factors that govern the role of the two conformational isomers and their packing systems.

A comparative study of the crystal structures of the complexes $[N^nBu_4][\{Mo(\eta^3\text{-}C_3H_5)(CO)_2\}_2(\mu\text{-}Cl)_2(\mu\text{-}OMe)]$ (**3**), $[PPN][\{Mo(\eta^3\text{-}C_3H_5)(CO)_2\}_2(\mu\text{-}Cl)_3]$ (**4**), $[Mo(CO)_2(\eta^3\text{-}C_3H_5)(MeCN)_3][\{Mo(\eta^3\text{-}C_3H_5)(CO)_2\}_2(\mu\text{-}Cl)_3]\cdot C_6H_6$ (**5**) and $[N^nBu_4][\{W(\eta^3\text{-}C_3H_5)(CO)_2\}_2(\mu\text{-}Cl)_3]$ (**6**) was carried out, and the coordinates were taken from the Cambridge Crystallographic database [12].

In the crystal structure of **3**, layers of $[\{Mo(\eta^3\text{-}C_3H_5)(CO)_2\}_2(\mu\text{-}Cl)_2(\mu\text{-}OMe)]^-$ anions are intercalated by layers of highly disordered *n*-butyl ammonium cations. The crystal structure of **5** is composed of layers of the complex species $[Mo(CO)_2(\eta^3\text{-}C_3H_5)(MeCN)_2]^+$ and $[\{Mo(\eta^3\text{-}C_3H_5)(CO)_2\}_2(\mu\text{-}Cl)_3]^-$ intercalated by layers of benzene solvent molecules. The solid-state structure of **6** is afforded by co-crystallization of $[\{W(\eta^3\text{-}C_3H_5)(CO)_2\}_2(\mu\text{-}Cl)_3]^-$ anions and ordered *n*-butyl ammonium cations. These two block units intercalate without a special structural crystal order, cations being surrounded by anions and vice-versa. The molecular assembling of anion $[\{Mo(\eta^3\text{-}C_3H_5)(CO)_2\}_2(\mu\text{-}Cl)_3]^-$ and PPN in **4** results in the most interesting solid-state structure of the group, as shown in Fig. 5. The $[Ph_3P{=}N^+{=}PPh_3]$ cation units are aggregate in layers, forming open double channels. Each one of these large channels accommodates two chains of $[\{Mo(\eta^3\text{-}C_3H_5)(CO)_2\}_2(\mu\text{-}Cl)_3]^-$ anions, which are related by a crystallographic inversion center. The channels are sheathed by C–H groups pointing towards the carbonyl groups of the anions.

We cannot draw conclusions from the different packing patterns in the two structures, because the change of isomer is accompanied by a drastic change of counterion. It is clear from Fig. 5 that the cations determine the main features of the crystal structure of **4**. Their presence is vital for forming the structure.

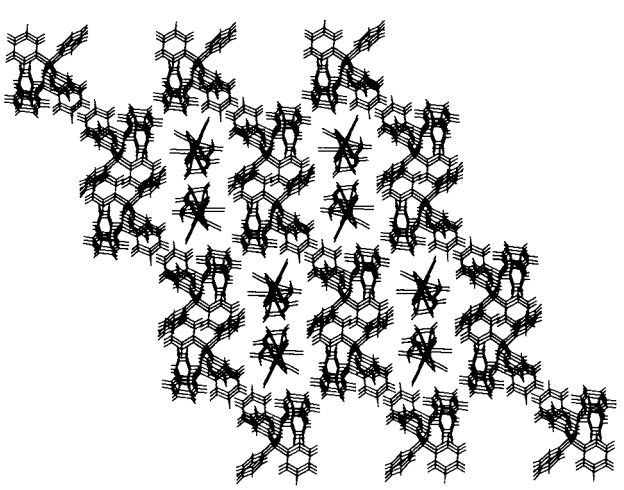

Fig. 5. Crystal packing diagram of **4** showing the open channels formed by PNP cations. These channels accommodate the complex anions.

3. Conclusions

The complex $[MoCl(\eta^3\text{-}C_3H_5)(CO)_2(H_2biim)]$ (**2**), with two N–H groups in the coordinated H_2biim ligand, appeared as a very promising precursor for the formation of molecular solids, different units being linked by hydrogen bonds. Such studies were unsuccessful, the main obstacle being its very poor solubility. On the other hand, we managed to isolated a different isomer of the well-known $[\{Mo(\eta^3\text{-}C_3H_5)(CO)_2\}_2(\mu\text{-}Cl)_3]^-$ anion, and showed, by means of both cyclic voltammetry and theoretical studies, that it does not interconvert into the other. The packing of the eclipsed isomer shows double chains of the dimer, but it is determined by the PPN cation, rather than the anion.

4. Experimental

4.1. Synthesis

Commercially available reagents and all solvents were purchased from standard chemical suppliers. All solvents were used without further purification except acetonitrile (dried over CaH_2), dichloromethane (dried over CaH_2), and THF, which was distilled over sodium–benzophenone ketyl and used immediately. 2,2′-Bisimidazole (H_2biim) [13] and $[(PMDTLi)_2biim$ [14] were synthesized according to literature procedures. ^{1}H-NMR spectra were recorded on a Bruker AMX-300 (300 MHz) spectrometer in acetone-d_6 (δ 2.04), CD_3CN (δ 1.93) and CD_3OD (δ 4.78 and 3.30) as solvents. Elemental analyses were carried out at ITQB and Universidade de Zaragoza (Perkin–Elmer 2400). The IR spectra were recorded on a Unicam Mattson 7000 FTIR spectrometer. Samples were run as KBr pellets.

4.2. Preparation of $[MoCl(\eta^3\text{-}C_3H_5)(CO)_2(H_2biim)]$ (**2**)

To a yellow solution of $[MoCl(\eta^3\text{-}C_3H_5)(CO)_2(NCMe)_2]$ in ethanol (0.311 g, 1 mmol) an equivalent amount of 2,2′-bisimidazole (0.134 g, 1 mmol) was added. After stirring overnight, an orange precipitate formed, which was isolated, washed with diethyl ether and dried under vacuum.

The yield was 0.276 g (76%). Anal. Calc. for $MoClC_{11}H_{11}N_4O_2$: C, 36.4; N, 15.4; H, 3.1. Found: C, 36.4; N, 15.3; H, 3.2%. ^{1}H-NMR (300 MHz, CD_3OD, 25°C): δ 7.63 (s, 2H, H_2biim), 7.48 (s, 4H, H_2biim), 4.09 (m, H, $H(allyl)_{meso}$); 3.52 (d, 2H, $H(allyl)_{syn}$); 1.41 (d, 2H, $H(allyl)_{anti}$).

4.3. Preparation of $[N^nBu_4][\{Mo(\eta^3\text{-}C_3H_5)(CO)_2\}_2(\mu\text{-}Cl)_2(\mu\text{-}OMe)]$ (**3**)

To a yellow solution of $[MoCl(\eta^3\text{-}C_3H_5)(CO)_2(NCMe)_2]$ in ethanol (0.622 g, 2 mmol) in 20 ml of freshly

distilled THF, [(PMDTLi)$_2$biim] (0.520 g, 1 mmol) was added. After refluxing for 2 h, the solution was filtered and evaporated to dryness. The remaining oil was redissolved in THF and [N^{n}Bu$_4$]Br was added (0.184 g, 2 mmol). The solution was filtered to separate excess [N^{n}Bu$_4$]Br and dried. The solid residue was recrystallized from methanol to give orange crystals. One crystal was studied by single-crystal X-ray diffraction.

The yield was 0.177 g (36%). ^{1}H-NMR (300 MHz, CD_3CN, 25°C): δ 3.08 (t, 8H, α N^{n}Bu$_4$); 1.59 (m, 8H, β N^{n}Bu$_4$); 1.35 (m, 8H, γ N^{n}Bu$_4$); 0.97 (t, 12H, δ N^{n}Bu$_4$).

4.4. Preparation of [PNP][{Mo(η^3-C_3H_5)(CO)$_2$}$_2$(μ-Cl)$_3$] (4)

A solution of [MoCl(η^3-C_3H_5)(CO)$_2$(NCMe)$_2$] in THF (0.031 g, 0.1 mmol) was cooled to 0°C in an ice bath. AuClPPN (0.081g, 0.1 mmol) was added. After it dissolved, the solution turned green. It was stirred for 30 min and filtered over celite. The volume of the yellow solution was reduced to 5 ml under vacuum and hexane was added. The green oil was converted to light green crystals after several additions of hexane. After recrystallization from hexane, light green crystals were obtained. One crystal was studied by single-crystal X-ray diffraction.

The yield was 0.091 g (87%). Anal. Calc. for $C_{46}H_{40}Cl_3O_4P_2NMo_2$: C, 53.6; N, 1,4; H, 3.9. Found: C, 52.9; N, 1.5; H, 3.8%. ^{1}H-NMR (300 MHz, CD_3CN, 25°C): δ 7.5–7.7 (m, 20H, PNP), 3.61 (m, H, H(allyl)$_{meso}$); 1.78 (s, 2H, H(allyl)$_{syn}$); 1.40 (s, 2H, H(allyl)$_{anti}$).

4.5. Crystal structure determinations

4.5.1. Crystal data

$C_{27}H_{49}Cl_2Mo_2NO_5$ (**3**), $M = 730.45$, triclinic space group, $P\bar{1}$, $a = 10.975(11)$, $b = 11.532(11)$, $c = 14.014(16)$ Å, $\alpha = 80.53(1)$ $\beta = 77.19(1)$, $\gamma = 89.64(1)°$, $V = 1705(3)$, $Z = 2$, $D_{calc.} = 1.423$ g cm^{-3}, $F(000) = 752$, $\mu = 0.924$ mm^{-1}.

$C_{46}H_{40}Cl_3Mo_2NO_4P_2$ (**4**), $M = 1030.96$, triclinic space group, $P\bar{1}$, $a = 10.060(14)$, $b = 15.360(17)$, $c = 16.750(17)$ Å, $\alpha = 117.04(1)$, $\beta = 95.31(1)$, $\gamma = 98.01(1)°$, $V = 2247(5)$ Å^3, $Z = 2$, $D_{calc.} = 1.524$ g cm^{-3}, $F(000) = 1040$, $\mu = 0.851$ mm^{-1}.

4.5.2. Data collection and processing

The X-ray single-crystal data for the two complexes were collected using graphite-monochromated Mo–K$_\alpha$ radiation on a MAR research image plate system ($\lambda = 0.71073$ Å) at Reading University. The crystals were positioned at 70 mm from the image plate. A total of 95 frames were measured at 2° intervals with a counting time suitable for the diffraction pattern exhibited by the complex under investigation. Data analysis was performed with the XDS program. [15] The intensities were not corrected for absorption effects.

4.5.3. Structure analysis and refinement

The positions of the molybdenum atoms were determined by direct methods and the positions of remaining non-hydrogen atoms were obtained subsequently by successive Fourier difference syntheses. The structures were refined by full-matrix least-squares methods on F^2 using a weighting scheme with the standard form.

For complex **4** 6871 independent reflections were measured, which were used in the solution and refinement of the structure. Anisotropic thermal parameters were used for all non-hydrogen atoms. The hydrogen atoms were introduced in the process refinement at ideal geometric positions with U_{iso} values equal to 1.2 times those of the atoms to which they were bonded. The final refinement converged to R and wR_2 values of 0.1061 and 0.2919 for the 4371 data with $I > 2\sigma(I)$ and 0.1921 and 0.3457 for all unique hkl data.

A total of 5445 independent reflections were measured for complex **3**, which are used in the structure solution and refinement calculations. From the earliest Fourier-difference maps calculated for this complex, it was apparent that the N^{n}Bu$_4$ cation was disordered. The refinement of a trial model including anisotropic thermal parameters for the nitrogen atom of the cation and all non-hydrogen atoms of the complex anion gave a high R value of 17% for the 2272 hkl data with $I > 2\sigma(I)$. Individual isotropic thermal parameters and unit occupation factors were considered for the carbon atoms of the N^{n}Bu$_4$ cation. For all these carbon atoms high values for the U_{iso} parameters were obtained, and other alternative positions were discernible for all atoms from the Fourier-difference map. These results indicated definitively that the N^{n}Bu$_4$ cation was strongly disordered. Then, many trial refinements were performed using different disorder models. Unfortunately, no trial model gave satisfactory results either in terms of a reasonable overall geometry for the N^{n}Bu$_4$ cation or a pronounced decrease of the R value. Consequently, the unsuccessful modeling of the contribution of N^{n}Bu$_4$ for the electronic density map led naturally to a low quality of the molecular structure of anion in **3**, namely in the standard deviations of their geometric parameters. However, the molecular geometry of the complex anion is unambiguous and allows us to compare the different stereochemistries of [{Mo(η^3-C_3H_5)(CO)$_2$}$_2$(μ-Cl)$_2$(μ-OMe)]$^-$ and [{Mo(η^3-C_3H_5)-(CO)$_2$}$_2$(μ-Cl)$_3$]$^-$.

All calculations required to solve and to refine the structures were carried out with SHELXS and SHELXL within the SHELX-97 package [16]. The molecular and crystal packing diagrams were drawn with PLATON [17].

4.6. Electrochemistry

The electrochemical instrumentation consisted of a BAS CV-50W voltammetric analyzer connected to BAS/Windows data-acquisition software. All the electrochemical experiments were run under argon at room temperature. Tetrabutylammonium hexafluorophosphate (Aldrich) was used as supporting electrolyte; it was recrystallized from ethanol. Cyclic voltammetry experiments were performed in a glass cell MF-1082 from BAS in a C-2 cell enclosed in a Faraday cage. The reference electrode was Ag | AgCl (MF-2079 from BAS) and its potential was −44 mV relative to a SCE. The reference electrode was calibrated with a solution of ferrocene (1 mM) to obtain a potential in agreement with the literature value [18]. The auxiliary electrode was a 7.5 cm platinum wire (MW-1032 from BAS) with a gold-plated connector. The working electrode was a platinum disk (MF-2013 from BAS) with ca. 0.022 cm^2 sealed in Kel-F plastic. Between each CV scan the working electrode was electrocleaned, polished on diamond 1 μM and alumina cleaning with water–methanol and sonicated before use, according to standard procedures. Solvents were dried as described previously.

4.7. DFT calculations

Density functional calculations [10] were carried out with the AMSTERDAM DENSITY FUNCTIONAL (ADF) program [11] developed by Baerends et al. (release 2.3) [19]. Vosko et al.'s local exchange correlation potential was used [20], with Becke's nonlocal exchange [21] and Perdew's correlation corrections [22]. Unrestricted calculations were performed for the paramagnetic complexes. The geometry optimization procedure was based on the method developed by Versluis and Ziegler [23], using the non-local correction terms in the calculation of the gradients. using nonlocal exchange and correlation corrections. The structures of the complexes described above and others referred to in the text were used to prepare input files for the full optimization of the geometry of the anionic complexes. In all the calculations, a triple-ζ Slater-type orbital (STO) basis set was used for Mo, 5s, 4p, 5p, 4d; triple-ζ STO augmented with a 3d single-ζ polarization function were used for C, 2s and 2p, O 2s and 2P, and H, 1s. A frozen core approximation was used to treat the core electrons of C (1s), O (1s), and Mo ([1–3]s, [1–3]p, 3d).

5. Supplementary material

Crystallographic data for the structural analyses have been deposited with Cambridge Crystallographic Data Centre, CCDC nos. 136832 for compound **3** and 136833 for compound **4**. Copies of this information may be obtained free of charge from The Director, CCDC, 12 Union Road, Cambridge CB2 1EZ, UK (Fax: +44-1223-336033; e-mail: deposit@ccdc.cam.ac.uk or www: http://www.ccdc.cam.ac.uk).

Acknowledgements

This work was supported by PRAXIS XXI under project PRAXIS/PCNA/C/QUI/103/96. We thank Zara Miravent Tavares for the elemental analysis (ITQB) and cyclic voltammetric experiments. P.P. thanks ITQB for a grant. M.J.C. and E.B. thank the TMR Transition Metal Clusters in Catalysis and Organic Synthesis. V.F. thanks the British Council and FCT for funding. The University of Reading and EPSRC are thanked for funds for the Image Plate system.

References

[1] (a) J.M. Lehn, Angew. Chem. Int. Ed. Engl. 29 (1990) 1304. (b) D. Braga, F. Grepioni, Acc. Chem. Res. 27 (1994) 51. (c) M.J. Calhorda, D. Braga, F. Grepioni, Transition metal clusters — the relationship between molecular and crystal structure, in: P. Braunstein, L.A. Oro, P.R. Raithby (Eds.), Metal Clusters in Chemistry, Wiley–VCH, Weinheim, 1999. (d) D. Braga, F. Grepioni, A.G. Orpen (Eds.), Crystal Engineering: from Molecules to Crystals, to Materials, Kluwer, Dordrecht, 1999.
[2] (a) D. Braga, M.J. Calhorda, F. Grepioni, P.E.M. Lopes, E. Tedesco, J. Chem. Soc. Dalton Trans. (1995) 1215. (b) C. Mealli, D.M. Proserpio, J. Organomet. Chem. 386 (1990) 203. (c) E. Hunstock, C. Mealli, M.J. Calhorda, J. Reinhold, Inorg. Chem. 38 (1999) 5053.
[3] (a) H. tom Dieck, H. Friedel, J. Organomet. Chem. 14 (1968) 375. (b) R.G. Hayter, J. Organomet. Chem. 13 (1967) P1. (c) P.K. Baker, Adv. Organomet. Chem. 40 (1996) 45 and references therein.
[4] C.G. Hull, M.H.B. Stiddard, J. Organomet. Chem. 9 (1967) 519.
[5] (a) H.D. Murdoch, R. Henzi, J. Organomet. Chem. 5 (1966) 552. (b) M.G.B. Drew, B.J. Brisdon, M. Cartwright, Inorg. Chim. Acta 36 (1979) 127.
[6] M. Boyer, J.-C. Daran, Y. Jeannin, Inorg. Chim. Acta 47 (1981) 191.
[7] C. Couldwell, K. Prout, Acta Crystallogr. Sect. B 34 (1978) 2439.
[8] F.A. Cotton, D.A. Ucko, Inorg. Chim. Acta 6 (1972) 161.
[9] B.J. Brisdon, K.A. Conner, R.A. Walton, Organometallics 2 (1983) 1159.
[10] R.G. Parr, W. Yang, Density Functional Theory of Atoms and Molecules, Oxford University, New York, 1989.
[11] AMSTERDAM DENSITY FUNCTIONAL (ADF) program, release 2.3, Vrije Universiteit, Amsterdam, The Netherlands, 1995.
[12] F.H. Allen, J.E. Davies, J.J. Galloy, O. Johnson, O. Kennard, C.F. Macrae, D.G. Watson, J. Chem. Inf. Comp. Sci. 31 (1991) 204.
[13] H. Debus, Ann. Chem. 197 (1858) 199.
[14] B.F. Fieselmann, D.N. Hendrickson, G.D. Stucky, Inorg. Chem 17 (1978) 2078.
[15] W. Kabsch, J. Appl. Crystallogr. 21 (1988) 916.

[16] G.M. Sheldrick, SHELX-97, University of Göttingen, Germany, 1997.
[17] A.L. Spek, PLATON, a Multipurpose Crystallographic Tool, Utrecht University, Utrecht, The Netherlands, 1999.
[18] I.V. Nelson, R.T. Iwamoto, Anal. Chem. 35 (1963) 867.
[19] (a) E.J. Baerends, D. Ellis, P. Ros, Chem. Phys. 2 (1973) 41. (b) E.J. Baerends, P. Ros, Int. J. Quantum Chem. S12 (1978) 169. (c) P.M. Boerrigter, G. te Velde, E.J. Baerends, Int. J. Quantum Chem. 33 (1988) 87. (d) G. te Velde, E.J. Baerends, J. Comp. Phys. 99 (1992) 84.
[20] S.H. Vosko, L. Wilk, M. Nusair, Can. J. Phys. 58 (1980) 1200.
[21] A.D. Becke, J. Chem. Phys. 88 (1987) 1053.
[22] (a) J.P. Perdew, Phys. Rev. B 33 (1986) 8822. (b) J.P. Perdew, Phys. Rev. B 34 (1986) 7406.
[23] (a) L. Versluis, T. Ziegler, J. Chem. Phys. 88 (1988) 322. (b) L. Fan, T. Ziegler, J. Chem. Phys. 95 (1991) 7401.